Received: 30 September 2019 | Revised: 3 July 2020 | Accepted: 7 July 2020

DOI: 10.1002/mus.27021

CLINICAL RESEARCH ARTICLE

MUSCLE&NERVE WILEY

Diffusion tensor imaging reveals changes in non-fat infiltrated muscles in late onset Pompe disease

Robert Rehmann MD[1] | Martijn Froeling PhD[2] | Marlena Rohm MSc[1] | Johannes Forsting[1] | Rudolf André Kley MD[1,3] | Tobias Schmidt-Wilcke MD[4,5] | Nesrin Karabul MD[6] | Christine H. Meyer-Frießem MD[7] | Jan Vollert PhD[8,9] | Martin Tegenthoff MD[1] | Matthias Vorgerd MD[1] | Lara Schlaffke PhD[1]

[1]Department of Neurology, Heimer Institute for Muscle Research, BG-University Hospital Bergmannsheil, Ruhr-University Bochum, Bochum, Germany

[2]Department of Radiology, University Medical Centre Utrecht, Utrecht, The Netherlands

[3]Department of Neurology, St. Marien-Hospital Borken, Borken, Germany

[4]St. Mauritius Therapieklinik, Meerbusch, Germany

[5]Institute of Clinical Neuroscience and Medical Psychology, University Hospital, University of Düsseldorf, Düsseldorf, Germany

[6]Endokrinologikum Frankfurt a. Main, Center of Hormonal and Metabolic Diseases, Rheumatology, Osteology and Neurology, Frankfurt a. M, Germany

[7]Department of Anaesthesiology Intensive Care Medicine and Pain Management, BG-University Hospital Bergmannsheil, Ruhr-University Bochum, Bochum, Germany

[8]Pain Research, Department of Surgery and Cancer, Imperial College, London, UK

[9]Neurophysiology, Center of Biomedicine and Medical Technology Mannheim CBTM, Medical Faculty Mannheim, Heidelberg University, Heidelberg, Germany

Correspondence
Lara Schlaffke, Department of Neurology, BG University Hospital Bergmannsheil, Ruhr-University Bochum, Bürkle-de-la-Camp-Platz 1, 44789 Bochum, Germany.
Email: lara.schlaffke@rub.de

Funding information
Genzyme, Grant/Award Number: GZ2015-11496; Sanofi.
Open access funding enabled and organized by Projekt DEAL.

Abstract

MRI is a helpful tool for monitoring disease progression in late-onset Pompe disease (LOPD). Our study aimed to evaluate if muscle diffusion tensor imaging (mDTI) shows alterations in muscles of LOPD patients with <10% fat-fraction. We evaluated 6 thigh and 7 calf muscles (both legs) of 18 LOPD and 29 healthy controls (HC) with muscle diffusion tensor imaging (mDTI), T1w, and mDixonquant sequences in a 3T MRI scanner. The quantitative mDTI-values axial diffusivity (λ_1), mean diffusivity (MD), radial diffusivity (RD), and fractional anisotropy (FA) as well as fat-fraction were analyzed. 6-Minute Walk Test (6-MWT) data were correlated to diffusion metrics. We found that mDTI showed significant differences between LOPD and HC in diffusion parameters ($P < .05$). Thigh muscles with <10% fat-fraction showed significant differences in MD, RD, and $\lambda_{1\text{-}3}$. MD positively correlated with 6-MWT ($P = .06$). To conclude, mDTI reveals diffusion restrictions in muscles of LOPD with and without fat-infiltration and reflects structural changes prior to fatty degeneration.

Abbreviations: 6-MWT, 6 Minute Walk Test; CK, creatine-kinase; ERT, enzyme replacement therapy; GAA, acid-alpha-glucosidase; λ_1, axial diffusivity; GSD II, glycogen storage disorder type II; HC, healthy control; LOPD, late-onset Pompe disease; mDTI, muscle diffusion tensor imaging; MRC, Medical Research Council; RD, radial diffusivity.

KEYWORDS
6-Minute Walk Test, diffusion tensor imaging, glycogen storage disease type II, magnetic resonance imaging, muscle, skeletal, tractography

1 | INTRODUCTION

Late-onset Pompe disease (LOPD) is an autosomal-recessive hereditary glycogen storage disorder glycogen storage disorder type II that leads to reduced or diminished function of the enzyme acid-alpha-glucosidase (GAA), causing tissue damage via lysosomal glycogen accumulation.[1,2] The skeletal muscle involvement is heterogeneous, affecting hamstring, paraspinal, and leg adductor muscles prior to others. Those muscles are also the first to show fatty degeneration in the lower body region in quantitative MRI sequences.[3-6] In order to monitor new therapeutic approaches and to identify disease activity in skeletal muscles non-invasively, sensitive and quantitative MR-imaging markers are essential. While T1w sequences show fat-infiltrated regions qualitatively, Dixon imaging sequences offer exact quantification of the amount of fat within a skeletal muscle due to chemical shift measurement and post processing algorithms.[7] In LOPD and dystrophic myopathies, Dixon imaging techniques measure fatty degeneration over time and are thereby able to quantify individual disease progression when fatty degeneration is already present.[3,6,8-12] Pathology of LOPD includes progressive glycogen and debris accumulation in skeletal muscles ultimately resulting in fatty degeneration. Imaging sequences that are both able to delineate possible disease-specific features prior to fatty degeneration and to quantify fat content are therefore of interest. Muscle diffusion tensor imaging (mDTI) can provide information about muscular microstructure and integrity by quantifying the directional diffusion properties of water molecules in muscle tissue.[13-15] By quantifying water diffusion in muscles, mDTI could provide additional sensitive information about microdamage.

mDTI has already shown disease-specific patterns of altered muscle architecture for various myopathies and identified changes of subclinical progression in hamstring muscles after long-distance running.[14,16,17] mDTI is thought to be of complementary value to quantitative MRI sequences, such as T2 mapping and Dixon fat quantification.[15,16,18,19] As mDTI highlights changes in water diffusion, it might also be of use in monitoring patients with LOPD, especially in providing additional information about muscles that do not yet show fatty degeneration.

In LOPD, mDTI has not yet been evaluated with regard to its ability to show disease-specific muscle diffusion alterations. Thus, the aims of our study were to: (a) evaluate if mDTI showed differences in diffusion metrics in the leg muscles of LOPD patients; (b) evaluate if mDTI showed alterations in muscles of LOPD patients with <10% fat-fraction. Those muscles normally appear "healthy" on conventional MR images. A deviance in mDTI parameters might then point toward a disease-specific muscle alteration. (c) Test if diffusion metrics correlated with 6-Minute Walk Test (6-MWT) data.

2 | METHODS

2.1 | Study design

This prospective study had been approved of by the local ethics committee of the Ruhr-University Bochum (No.: 15–5281) and written informed consent was obtained from all participants prior to enrollment.

The inclusion criterion for the LOPD cohort was a genetically confirmed diagnosis of LOPD. Exclusion criteria were contraindications for MRI examination and other co-existing neuromuscular diseases. Healthy controls were recruited within the working environment of the research group. Some members of the healthy control cohort served as controls for another recent study by our group.[20] Each participant was examined clinically by an experienced neurologist.

2.2 | Clinical evaluation

Each extremity was tested for strength based on the Medical Research Council (MRC) grading scale by a clinical neurologist with the patients supine. The following movements were tested for each leg individually: hip flexion, hip extension, knee flexion, knee extension, ankle dorsiflexion, and ankle plantar flexion. The MRC mean value for both legs combined is presented as "muscle strength". The 6-Minute Walk Test (6-MWT) was performed after the MRI scan by an experienced medical technical assistant. Participants were asked to walk as fast as possible (no jogging or running) during a time-span of 6 min circling the standardized track in our gym according to the guideline for the 6-MWT.[21] The distance was measured in meters / 6 min.

The results of the 6-MWT were compared with previously obtained 6-MWT data of the same age range. We calculated the distance of a healthy person in the 6-MWT according to Troosters et al. using the following equation[22]:

$$6-\mathrm{MWT}_{\mathrm{pred}} = 218 + (5.14 * \mathrm{height} * 100 - 5.32 * \mathrm{age}) - (1.8 * \mathrm{weight} + 51.31 * \mathrm{gender}).$$

$$\mathrm{Male} = 1, \mathrm{Female} = 0.$$

2.3 | MRI protocol

MRI was performed using a 3T MRI (Achieva 3T X, Philips medical Systems) and a 16-channel Torso coil (Philips TorsoXL). The thigh region from hip to knee was divided into three fields of view (FOV) of 480x264x150 mm^3 along the z-axis (stacks) to avoid shimming artifacts occurring due to large FOV. The stacks had a 10 mm overlap to

TABLE 1 Demographic and clinical data of the patient cohort

Patient	Age (years)	Height (meters)	Weight (kg)	BMI (kg/m^2)	Sex (m = 10)	Muscle strength (MRC)	Months since diagnosis	Enzyme replacement therapy duration (months)	6-MWTin meters (m)	Predicted 6-MWT in meter (m) (6-MWTPred)
1	57	1.86	82	24	m	4.67	120	100	540 m	698
2	54	1.92	72	20	m	3.92	84	84	N.a.	N.a.
3	47	1.73	63	21	f	5	60	36	404 m	654
4	47	1.81	84	26	m	4.75	22	18	459 m	728
5	32	1.71	52	18	m	4.50	312	119	504 m	773
6	46	1.71	65	22	f	4.75	43	40	486 m	657
7	16	1.7	50	17	m	5	84	60	675 m	821
8	55	1.89	85	24	m	5	15	8	594 m	704
9	19	1.67	65	23	f	5	120	71	675 m	737
10	71	1.69	85	30	f	4.67	8	8	N.a.	N.a.
11	50	1.86	78	23	m	4.67	2	2	344 m	719
12	27	1.71	68	23	f	5	11	None	522 m	713
13	30	1.87	93	27	m	5	47	39	450 m	779
14	29	1.61	57	22	f	5	N.a.	N.a.	648 m	707
15	18	1.8	95	29	m	5	16	None	540 m	815
16	42	1.88	65	18	m	4.92	324	131	N.a.	N.a.
17	26	1.6	57	22	f	5	N.a.	N.a.	448 m	716
18	32	1.73	103	34	f	4.83	41	38	256 m	698
Mean (SD)	38.8 (±15.5)	1.76 (0.10)	73.3 (15.5)	23.5 (4.4)		4.81 (0.28)	81.8 (99.5)	53.8 (41.8)	503 (118)	728 (50)

Abbreviations: 6-MWT, 6-Minute Walk Test; MRC, Medical Research Council Scale; N.a., data not assessed, f , female, m, male.

allow accurate merging. The MRI acquisition protocol for each FOV comprised T1-weighted (T1w), T2-weighted (T2w), diffusion weighted imaging (DWI), as well as one noise measurement (by turning off the RF and imaging gradients), with a total acquisition time of approximately 27 min for both thighs (9 min per FOV).[17,20,23] In addition, a Dixon fat-quantification sequence (mDixonquant) was acquired. After the image acquisition of the thigh-regions, the data acquisition was paused, and the coil was wrapped around the lower leg region; scanning continued afterward.

The lower leg region was divided into two FOVs with the same imaging protocol as used for thighs with a total acquisition time of approximately 18 min for both lower legs (9 min per FOV). See Table S1 for acquisition details.

2.4 | Data processing

Data were processed using QMRITools (github.com/mfroeling/QMRITools running under *Mathematica 11*). Data preprocessing was performed akin to Schlaffke et al.[23] T1w and T2w data of the individual stacks were corrected for motion between the stacks using rigid registration of the overlapping slices. Diffusion data were denoised using a principal component analysis method.[24] Next, the diffusion data was corrected for subject motion and eddy current distortions by using affine registration and aligned to T2-data by using non-rigid registration. Finally, the aligned and corrected T1w, T2w and DWI data were fused by weighted averaging of the overlapping slices, yielding one volume covering the entire thighs and calves.

The diffusion tensor was estimated from the corrected and merged diffusion data using an iWLLS tensor estimation with outlier detection.[25] From the tensor, the three eigenvectors $\nu_{1\text{-}3}$ and their scalar, the eigenvalues λ_1-λ_3, were calculated for each voxel. Fractional anisotropy (FA) and mean diffusivity (MD) were calculated based on the three eigenvalues.

The mDixonquant sequence allows the online reconstruction of fat-fraction maps directly on the MR host computer.

2.5 | Tractography

Whole leg deterministic tractography was performed akin to Basser et al. using the Matlab based ExploreDTI toolbox.[26,27] A seed grid of 3x3x3 mm^3 was used to start deterministic tractography. Fibers were terminated if FA was lower than 0.1 or higher than 0.6, angle between 2 tensors was higher than 15°, or step size between to tensors was higher 1.5 mm.[17,23]

2.6 | Muscle segmentation

In total, six thigh and seven calf muscles were segmented. Thigh: vastus lateralis, vastus medialis, rectus femoris, biceps femoris (long and short head), semimembranosus, semitendinosus. calf: extensor digitorum longus, gastrocnemius lateralis and medialis, soleus, peroneus (peroneus longus and brevis), tibialis anterior and posterior. Segmentation was performed via (a) tractography and (b) manually using T1 data. Based on whole leg tractography, the six thigh and seven calf muscles were manually segmented using "seed" and "not" gates, to obtain tractography data (λ_1, MD, RD, FA) for each muscle separately.[23]

Manual segmentation of all muscles was performed based on the T1w images by drawing regions of interest (ROIs) on every slice of the T1 weighted data set to generate muscle specific masks. This was done by a single examiner. The resulting masks were subsequently eroded by one voxel to avoid including fascia. The masks derived were superimposed on mDixonquant fat-fraction maps (if available) to obtain muscle specific fat-fractions. Whole thigh and calf fat-fraction data were calculated as the mean of the average fat-fraction of the individual muscles.

2.7 | Statistical analyses

Available fat-fractions were compared between LOPD patients and healthy controls in a general linear model with patient/control, body side, and muscle (to control degrees of freedom for multiple test points per subject) as fixed factors for thigh and calf muscles separately.

The mDTI parameters λ_1, MD, RD, and FA were analyzed in a multivariate general linear model with patient/control, body side, and muscle as fixed factors. In a subsequent analysis, all muscles with a fat-fraction higher than 10% (or without assessed fat-fraction) were excluded, to evaluate the diffusion differences between controls and low-fat LOPD muscles.

Muscle fat-fraction values in the low-fat analysis were compared between healthy controls and LOPD to show an equal FF distribution in all muscles between groups.

The cutoff value for all low-fat muscles was based on the healthy control group. The highest fat content in the control group was detected in the biceps femoris muscle with 7.1% (SD of 3.2%). Thus,

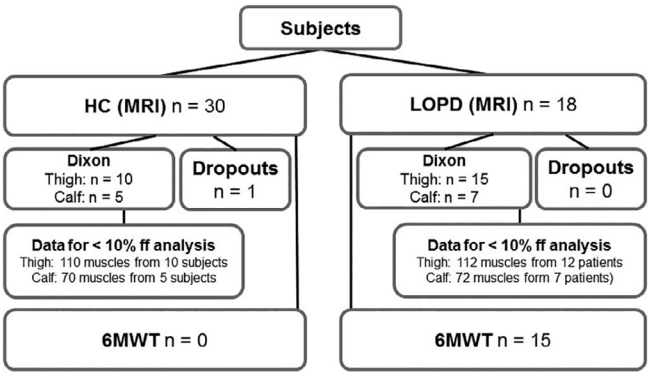

FIGURE 1 Number of healthy controls (HC) and late onset pompe disease (LOPD) patients with Dixon imaging and 6 minute walk test (6-MWT). 6-MWT and number of cases used for the low-fat analysis (ff = fat-fraction)

TABLE 2 Diffusion and acquired fat-fraction data for patients and controls

Upper leg											
	Control - all			LOPD - all				Control < 10% ff		LOPD < 10% ff		
Muscle	Diff *N*	Fat *N*	Fat mean ± SD (min - max)	Diff *N*	Fat *N*	Fat mean ± SD (min - max)	*P*	Fat *N*	Fat mean ± SD (min - max)	Fat *N*	Fat mean ± SD (min - max)	*P*
VL	58	20	4.4 ± 2.3 (2–10.2)	36	30	11.6 ± 14.2 (1.9–50)	.01*	*19*	*4.1 ± 1.9 (2–9.2)*	22	4.3 ± 2 (1.9–9.2)	.67
VM	57	20	4.1 ± 1.3 (2.4–6.5)	35	30	15.9 ± 20.5 (1.9–79.2)	.004*	*20*	*4.1 ± 1.3 (2.4–6.5)*	19	4.7 ± 1.9 (1.9–8.4)	.286
RF	58	20	3.4 ± 1.1 (1.6–5.4)	36	30	8.1 ± 8.6 (1.2–33.3)	.006*	*20*	*3.4 ± 1.2 (1.6–5.4)*	23	3.9 ± 2.2 (1.2–9.5)	.364
SM	58	20	6.3 ± 2.2 (3.1–11.1)	35	30	24.9 ± 2.4 (2.3–78.2)	<.001*	*18*	*5.8 ± 1.8 (3.1–9.3)*	14	5.1 ± 2.5 (2.3–10)	.364
ST	58	20	5.7 ± 2.2 (3.3–10.5)	36	30	11.6 ± 11.9 (2.2–47.7)	.013*	*19*	*5.4 ± 2 (3.3–9.3)*	22	5.4 ± 1.9 (2.2–8.8)	.98
BF	58	20	7.1 ± 3.1 (4.4–15.9)	36	30	20.2 ± 20 (2.5–69.6)	.001*	*16*	*5.8 ± 1.6 (4.4–9.9)*	14	5.2 ± 1.9 (2.5–9.2)	.381
ALL	*347*	*120*	*5.2 ± 2.5 (1.6–15.9)*	*214*	*180*	*15.4 ± 18 (1.2–79.2)*	<.001*	*112*	*4.7 ± 1.9 (1.6–9.9)*	*114*	*4.7 ± 2.1 (1.2–10)*	.982
Lower leg												
Muscle	Diff N	Fat N	Fat mean ± SD (min - max)	Diff N	Fat N	Fat mean ± SD (min - max)	P	Fat N	Fat mean ± SD (min - max)	Fat N	Fat mean ± SD (min - max)	*P*
MGM	34	10	3.8 ± 0.9 (2.2–5)	54	14	11.4 ± 14 (0.2–44.7)	.067	10	3.8 ± 0.9 (2.2–5)	9	3.4 ± 1.9 (0.2–5.7)	.548
LGM	34	10	4.1 ± 1.1 (2.5–5.5)	54	14	6.7 ± 6.3 (0.1–23.1)	.158	10	4.1 ± 1.1 (2.5–5.5)	12	4.5 ± 3 (0.1–9.2)	.685
SOL	34	10	4.5 ± 0.8 (3.1–5.7)	54	14	6 ± 2.4 (2.5–11)	.042*	10	4.5 ± 0.8 (3.1–5.7)	13	5.6 ± 2 (2.5–8.5)	.107
TA	34	10	3.2 ± 1.2 (1.8–5)	53	14	10.9 ± 16.3 (1.6–59.7)	.1	10	3.2 ± 1.2 (1.8–5)	10	3.9 ± 1.7 (1.6–7.1)	.358
PM	34	10	5.5 ± 1.3 (3.3–7.4)	54	14	12.8 ± 11 (2.6–46.3)	.028*	10	5.5 ± 1.3 (3.3–7.4)	7	6.6 ± 2.7 (2.6–9.4)	.249
EDL	34	10	2.7 ± 0.9 (1.6–4)	54	14	9.4 ± 10.4 (1.6–37.1)	.033*	10	2.7 ± 0.9 (1.6–4)	10	4.6 ± 2.8 (1.6–9.6)	.064
TP	34	10	2.8 ± 0.8 (1.8–4.5)	54	14	6 ± 4.3 (1.4–15.3)	.015*	10	2.8 ± 0.8 (1.8–4.5)	11	4.2 ± 2.3 (1.4–9.2)	.09
ALL	238	*70*	*3.8 ± 1.3 (1.6–7.4)*	*377*	*98*	9 ± 10 (0.1–59.7)	<.001*	*70*	*3.8 ± 1.3 (1.6–7.4)*	*72*	4.7 ± 2.5 (1.5–9.6)	.013*

Abbreviations: VL = vastus lateralis; VM = vastus medialis;RF = rectus femoris; SM = semimebranosus, ST = semiteninosus; BF = biceps femoris; MGM = medial gastrocnemius; LGM = lateral gastrocnemius; SOL = soleus; TA = tibialis anterior; PM = peroneal; EDL = extensor digitorum longus; TP = tibialis posterior, ff = fat-fraction. P: significance level for unpaired t-tests.

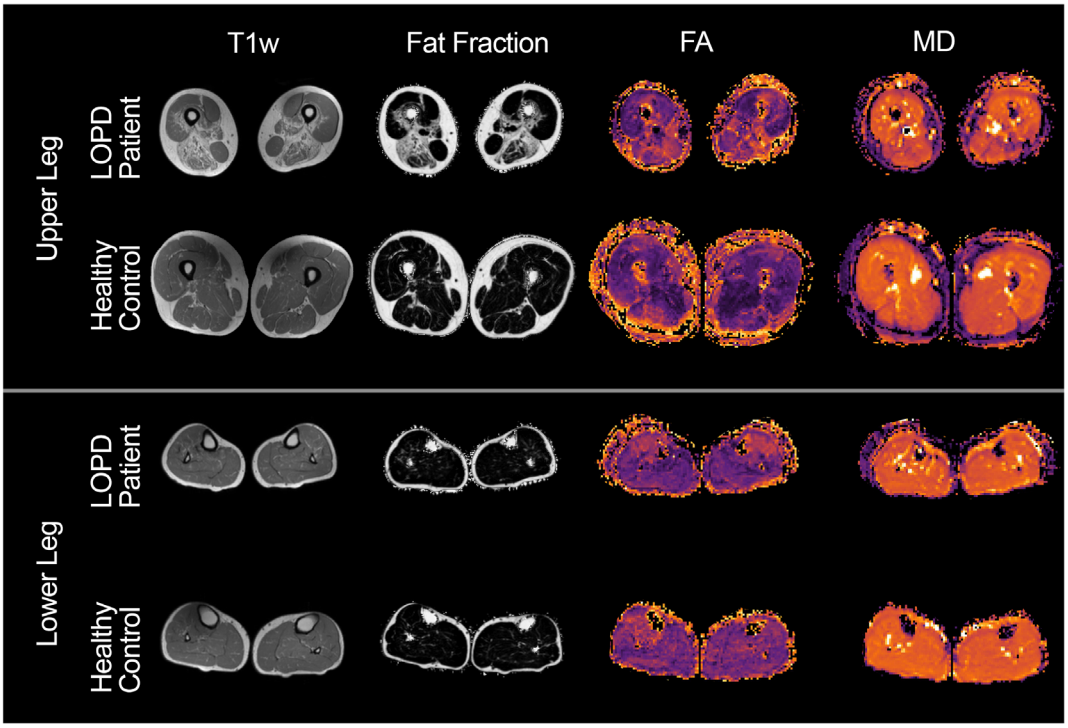

FIGURE 2 Example images of the applied MRI sequences. Upper leg: axial slices of MR images; proximal thigh muscles of late onset pompe disease (LOPD) patient and healthy control (HC). MRI sequences from left to right: T1w, mDixon fat-fraction, fractional anisotropy (FA), mean diffusivity (MD). T1w, mDixon, FA, and MD map show fatty infiltration and signal alteration in posterior thigh muscle compartment. Lower leg: axial slices of MR images; proximal calf muscles of LOPD patient and HC. No visible alterations [Color figure can be viewed at wileyonlinelibrary.com]

the cutoff value was defined as follows: highest mean fat-fraction in healthy controls +1x SD: ~ 10%.

Significance level was set to $P < .05$ and adjusted for multiple comparisons using the Benjamini-Hochberg procedure. All diffusion parameters of all thigh muscles were correlated to the 6-MWT data using Pearson´s r correlation coefficients.

3 | RESULTS

3.1 | Study participants

In the LOPD group there were 8 females and 10 males (mean age 38.7 years, range: 16–71 yrs). The control cohort was composed of 15 females and 15 males (mean age 31.1 years, range: 21–53 years).

For demographic and clinical data of the LOPD patients, see Table 1. Body measures of the control group and the LOPD patients are summarized and compared in the Supplementary Information Table S2, which is available online.

Muscle strength analysis revealed normal muscle strength for all healthy controls (5/5 on MRC scale) and slightly reduced strength (4.8/5) for LOPD patients (see Table 1 for details). One healthy control had to be excluded from the analysis due to motion artifacts. The dixon fat-quantification (Dixonquant) was successfully acquired for the thigh muscles in ten healthy controls and 15 LOPD patients. Due to water-fat swaps (errors in the reconstruction) we had to exclude five calf data sets from healthy controls and eight calf datasets for LOPD patients (see Figure 1). The average fat-fraction was significantly higher in both calf and thigh muscles in patients than in controls. See Table 2 for detailed fat-fraction data.

A representative T1w image, as well as a fat-fraction map, an FA map and an MD map of a LOPD patient and a matched control are shown in Figure 2. All diffusion parameters were significantly different between patients and controls in the thigh muscles. In the calf, all parameters except for FA showed a significant difference (Table 3).

When comparing only muscles with less than 10% fat-fraction, all diffusion parameters except FA showed significant differences in the thigh muscles, whereas the signal to noise ratio in these muscles, which was estimated based on the noise measures, was comparable between groups: control 19–62, mean 41.7 ± 9; LOPD 17–64, mean 40.0 ± 8 ($P = .166$). None of the diffusion parameters (except FA) showed a significant correlation with the fat-fraction. No significant differences in diffusion metrics were found in the calf muscles with<10% fat-fraction (Table 3).

Figure 3 shows the mean values of the diffusion parameters of the individual low-fat thigh muscles. Mean and radial diffusivity were significantly higher in controls than patients in some of the thigh muscles (see Figure 3). The MD of the thigh muscles revealed a moderately positive correlation with the walking distance (in meters) achieved during the 6-MWT (see Figure 4). Other diffusion parameters did not show a significant correlation.

TABLE 3 Diffusion metrics for controls and patients

Upper leg	All controls (n = 29)	All patients (n = 18)	*P*	Controls ff < 10% (n = 10)	Patients ff < 10% (n = 12)	*p*
λ_1	2.05 ± 0.12	1.97 ± 0.13	<.0001*	2.05 ± 0.11	1.99 ± 0.11	.001*
MD	1.67 ± 0.09	1.60 ± 0.11	<.0001*	1.67 ± 0.08	1.62 ± 0.08	.002*
RD	1.49 ± 0.09	1.42 ± 0.11	<.0001*	1.48 ± 0.08	1.44 ± 0.07	.010*
FA	0.20 ± 0.03	0.21 ± 0.03	<.0001*	0.21 ± 0.03	0.20 ± 0.03	.325
Lower leg	All controls (n = 29)	All patients (n = 18)	*P*	Controls Ff < 10% (n = 5)	Patients Ff < 10% (n = 7)	*P*
λ_1	2.08 ± 0.15	2.04 ± 0.16	.003*	2.02 ± 0.18	2.05 ± 0.17	.214
MD	1.70 ± 0.13	1.66 ± 0.12	<.0001*	1.66 ± 0.10	1.66 ± 0.17	.879
RD	1.51 ± 0.12	1.49 ± 0.17	.007*	1.48 ± 0.10	1.50 ± 0.12	.475
FA	0.20 ± 0.02	0.20 ± 0.02	.541	0.20 ± 0.03	0.20 ± 0.02	.180

Note: P-Values are derived from general linear models with disease/control as fixed factor, controlled for muscle and body side as fixed factors. The unit for λ1, RD, and MD is 10^{-3} mm^2/s.
*Significant on $P < .05$, corrected for multiple testing using the Benjamini-Hochberg procedure.
Abbreviations: λ1, Lambda 1; RD, radial diffusivity; MD, mean diffusivity; FA, fractional anisotropy; ff, fat-fraction.

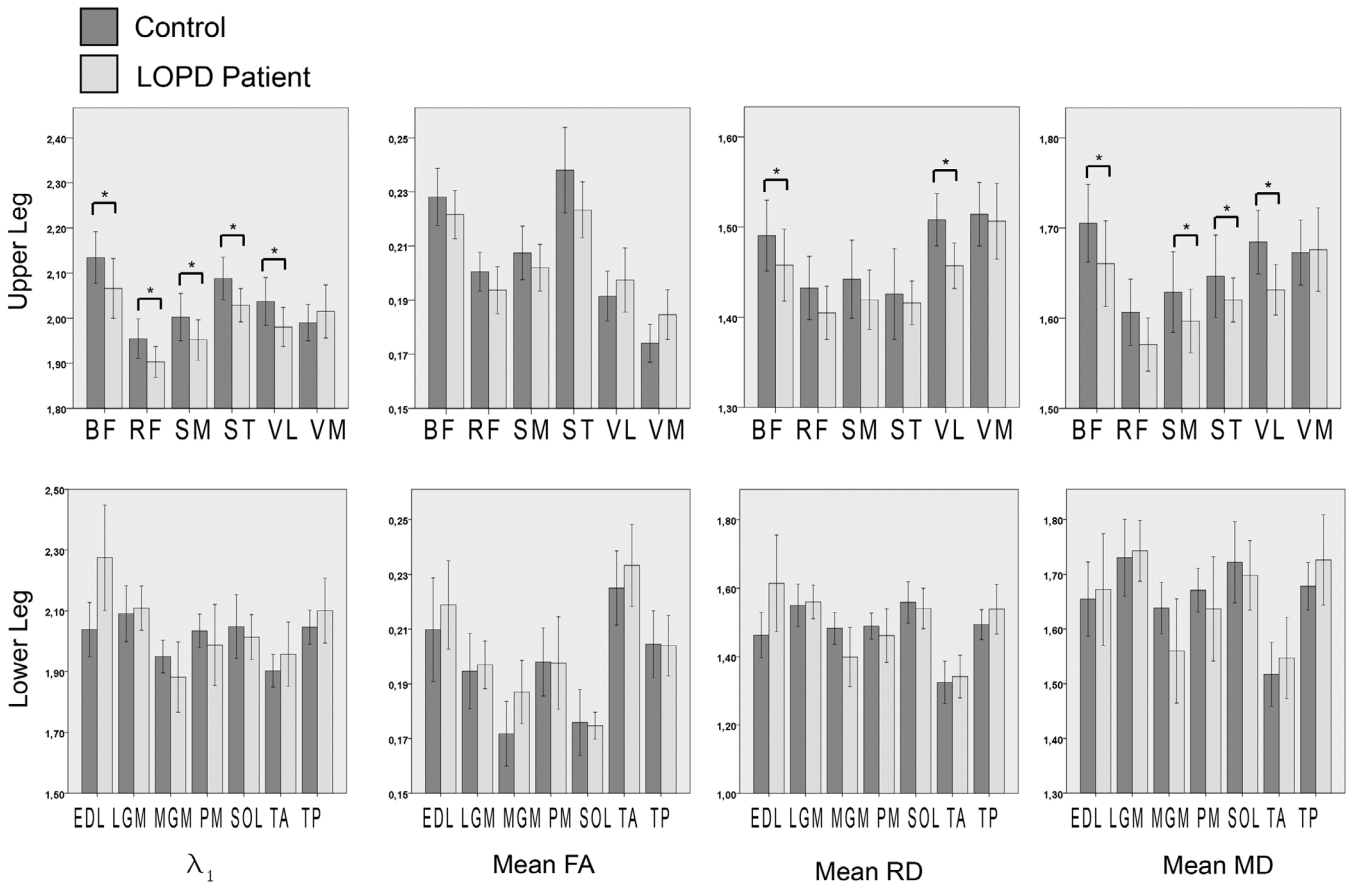

FIGURE 3 Diffusion metrics of thigh muscles with fat-fraction <10%. λ1, lambda 1; RD, radial diffusivity; MD, mean diffusivity; FA, fractional anisotropy; VL, vastus lateralis; VM, vastus medialis; RF, rectus femoris; SM, semimebranosus; ST, semiteninosus; BF, biceps femoris; MGM, medial gastrocnemius; LGM, lateral gastrocnemius; SOL, soleus; TA, tibialis anterior; PM, peroneal; EDL, extensor digitorum longus; TP, tibialis posterior. Asterisks indicate significant post-hoc t-test ($P < .05$)

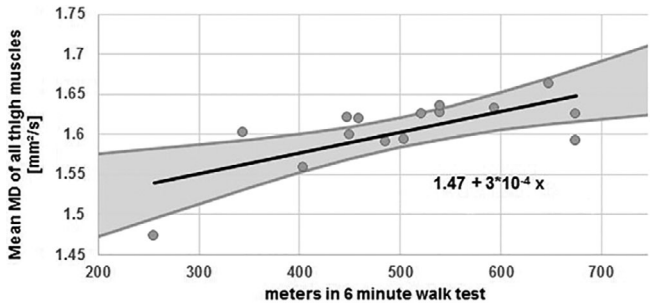

FIGURE 4 Correlation of the mean diffusivity and 6-Minute Walk Test (6-MWT) of all patients thigh muscles to the distance covered in the 6-MWT. R = 0.686, *P* = .003. MD, mean diffusivity

4 | DISCUSSION

The significant alteration of mDTI metrics in all thigh and calf muscles (except for FA) confirms that muscles with medium to advanced fatty degeneration in mDixon imaging and T1w images are impaired in diffusion imaging. The lack of differences in FA between the groups is most likely due to the lower sensitivity of FA compared with MD. The FA reflects a scalar value between 0 and 1, whereas the MD reflects the actual mean diffusivity of the estimated tensor.

Furthermore, thigh muscles with a fat-fraction of <10% showed a significant reduction in mDTI metrics compared to the healthy control group, although this could not be shown for calf muscles. MD values moderately correlated with 6-MWT data.

MD reflects the local amount of water diffusion.[19] Thus, it is elevated in muscles with cellular edema, increased membrane permeability, or hypertrophy. MD is decreased in muscles with structural damage, scar tissue, fatty infiltration, and atrophy. We were able to demonstrate that MD is decreased in all thigh and calf muscles of LOPD patients.[13,18,19,28-30]

The LOPD muscles with <10% fat-fraction also showed decreased MD with no muscle fiber atrophy, since this would be accompanied by an increase in FA with a relative increase of λ_1 compared to λ_2 and λ_3.[19]

The reduction observed in the low-fat muscles indicates muscle degeneration prior to significant fatty replacement. This would be in line with the pathophysiology of LOPD muscles, where there are intracellular debris and enlarged lysosomes prior to fatty degeneration.

Our results are well in line with other studies. Keller et al. analysed DTI metrics in a group of patients with different muscular dystrophies. They showed that DTI metrics were already altered in regions of leg muscles that were not affected by fatty infiltration and observed that fatty infiltration in turn intensified this effect. They concluded that mDTI could reveal structural muscle damage due to dystrophic degeneration.[18]

In our study, we observed alterations of mDTI metrics predominantly in the hamstring muscles and showed an intermuscular gradient in terms of MD, RD and λ_{1-3}, ranging from higher MD values in the anterior thigh muscle compartment to lower MD values in the hamstring muscles.

Our results of the distribution of altered mDTI parameters are also in line with recently published data on other quantitative MRI sequences in LOPD and indicate that diffusion imaging can be used to identify patterns of disease progression and early muscle involvement. Early involvement of the hamstring muscles was also shown by others.[3,6,31] A reduction in MD in the hamstring muscles, therefore, could precede fatty degeneration and serve as a marker for advanced intracellular debris accumulation.

Both postulated conclusions about possible microstructural alterations should be validated in future studies with a longitudinal study design and validation by muscle biopsies.

Our data revealed a significant positive correlation of the mean MD of all thigh muscles with the distance covered in 6-MWT. The distance covered in 6 min by LOPD patients was significantly shorter compared to the estimated data for healthy controls and in line with previously reported data.[32] This difference is due mainly to the disease and to age related variations, as age was also included as a factor in the predicted distance. Although the correlation between 6MWT and MD was moderate (r = 0.686), it supports a connection between functional muscle testing and quantitative MRI data. Further studies should evaluate correlations between upper leg muscle strength and functional muscle testing.

Regarding study limitations, our sample size is relatively small, largely due to the rarity of LOPD. The data were collected in a single center and acquired over 2 years. We did not perform muscle biopsies; thus, we cannot compare our results with histopathologic data. We cannot fully exclude age as a confounding factor for some amount of reduction in MD. Future studies should include larger sample sizes and a broader age distribution among subjects. To investigate whether our results are based on glycogen accumulation, future studies should include measurements of glycogen either by muscle biopsy or noninvasive methods, such as glycoCEST.[33]

We conclude that mDTI metrics, especially MD, particularly when combined with quantitative MRI sequences already in use, can make an important contribution in evaluating both disease-specific changes and disease progression in the skeletal muscles of patients with LOPD. The mDTI parameters revealed diffusion restrictions in muscles with no fatty infiltration, likely reflecting the underlying disease pathology of intracellular debris accumulation and lysosome enlargement.

ACKNOWLEDGEMENTS

This basic research study was funded by Sanofi-Genzyme with a research grant (GZ-15-11496). Grant applicants were Robert Rehmann, Tobias Schmidt-Wilcke, Matthias Vorgerd. We thank Philips Germany, especially Burkhard Maedler for continuous scientific support. Open access funding enabled and organized by Projekt DEAL.

CONFLICTS OF INTERESTS

None of the authors has any conflict of interest to disclose.

ETHICAL PUBLICATION STATEMENT

We confirm that we have read the Journal's position on issues involved in ethical publication and affirm that this report is consistent with those guidelines.

ORCID

Martijn Froeling https://orcid.org/0000-0003-3841-0497

Christine H. Meyer-Frießem https://orcid.org/0000-0001-8743-2065

Jan Vollert https://orcid.org/0000-0003-0733-5201

Lara Schlaffke https://orcid.org/0000-0002-0716-3780

REFERENCES

1. Lim JA, Li L, Raben N. Pompe disease: from pathophysiology to therapy and back again. *Front Aging Neurosci*. 2014;6:1-14.
2. Schüller A, Wenninger S, Strigl-pill N, Schoser B. Toward deconstructing the phenotype of late-onset Pompe disease. *Am J Med Genet Part C*. 2012;9:80-88.
3. Carlier PG, Azzabou N, De Sousa PL, et al. Skeletal muscle quantitative nuclear magnetic resonance imaging follow-up of adult Pompe patients. *J Inherit Metab Dis*. 2015;38:565-572.
4. Carlier RY, Laforet P, Wary C, et al. Whole-body muscle MRI in 20 patients suffering from late onset Pompe disease: involvement patterns. *Neuromuscul Disord*. 2011;21(11):791-799.
5. Do HV, Khanna R, Gotschall R. Challenges in treating Pompe disease: an industry perspective. *Ann Transl Med*. 2019;7(13):291-291.
6. van der Ploeg A, Carlier PG, Carlier RY, et al. Prospective exploratory muscle biopsy, imaging, and functional assessment in patients with late-onset Pompe disease treated with alglucosidase alfa: the EMBASSY study. *Mol Genet Metab*. 2016;119(1–2):115-123.
7. Dixon WT. Simple Proton Spectroscopic Imaging. *Radiology*. 1984;153:189-194.
8. Horvath JJ, Austin SL, Case LE, et al. Correlation between quantitative whole-body muscle magnetic resonance imaging and clinical muscle weakness in pompe disease. *Muscle Nerve*. 2015;51(5):722-730.
9. Willis TA, Hollingsworth KG, Coombs A, et al. Quantitative muscle MRI as an assessment tool for monitoring disease progression in LGMD2I: a multicentre longitudinal study. *PLoS One*. 2013;8(8):6-12.
10. Figueroa-Bonaparte S, Segovia S, Llauger J, et al. Muscle MRI findings in childhood/adult onset pompe disease correlate with muscle function. *PLoS One*. 2016;11(10):1-19.
11. Morrow JM, Sinclair CDJ, Fischmann A, et al. MRI biomarker assessment of neuromuscular disease progression: a prospective observational cohort study. *Lancet Neurol* [Internet. 2016;15(1):65-77.
12. Carlier PG, Marty B, Scheidegger O, et al. Skeletal muscle quantitative nuclear magnetic resonance imaging and spectroscopy as an outcome measure for clinical trials. *J Neuromuscul Dis*. 2016;3(1):1-28. http://www.medra.org/servlet/aliasResolver?alias=iospress&doi=10.3233/JND-160145.
13. Budzik J-F, Balbi V, Verclytte S, Pansini V, Le TV, Cotten A. Diffusion tensor imaging in musculoskeletal disorders. *Radiographics*. 2014;34(3):E56-E72.
14. Damon B, Li K, Bryant ND. Magnetic resonance imaging of skeletal muscle disease. *Handb Clin Neurol*. 2016;136(3):827-842.
15. Oudeman J, Nederveen AJ, Strijkers GJ, Maas M, Luijten PR, Froeling M. Techniques and applications of skeletal muscle diffusion tensor imaging: a review. *J Magn Reson Imaging*. 2016;43(4):773-788.
16. Damon BM, Froeling M, Buck AKW, et al. Skeletal muscle diffusion tensor-MRI fiber tracking: rationale, data acquisition and analysis methods, applications and future directions. *NMR Biomed*. 2016;30(e3563):1-13.
17. Froeling M, Oudeman J, Strijkers GJ, et al. Muscle changes detected with diffusion-tensor imaging after long-distance running. *Radiology*. 2015;274(2):548-562.
18. Keller S, Wang ZJ, Aigner A, et al. Diffusion tensor imaging of dystrophic skeletal muscle: comparison of two segmentation methods adapted to chemical-shift-encoded water-fat MRI. *Clin Neuroradiol*. 2019;29(2):231-242.
19. Berry DB, Regner B, Galinsky V, Ward SR, Frank LR. Relationships between tissue microstructure and the diffusion tensor in simulated skeletal muscle. *Magn Reson Med*. 2018;80(1):317-329.
20. Rehmann R, Schlaffke L, Froeling M, et al. Muscle diffusion tensor imaging in glycogen storage disease V (McArdle disease). *Eur Radiol*. 2018;29(6):3224-3232.
21. American Thoracic Society. ATS statement: guidelines for the six-minute walk test. *Am J Respir Care Med*. 2002;166:111-117.
22. Troosters T, Gosselink R, Decramer M. Six minute walking distance in healthy elderly subjects. *Eur Respir J*. 1999;14(2):270-274.
23. Schlaffke L, Rehmann R, Froeling M, et al. Diffusion tensor imaging of the human calf: variation of inter- and intramuscle-specific diffusion parameters. *J Magn Reson Imaging*. 2017;46(4):1137-1148.
24. Veraart J, Novikov DS, Christiaens D, Ades-aron B, Sijbers J, Fieremans E. Denoising of diffusion MRI using random matrix theory. *Neuroimage*. 2016;142:394-406.
25. Veraart J, Sijbers J, Sunaert S, Leemans A, Jeurissen B. Weighted linear least squares estimation of diffusion MRI parameters: strengths, limitations, and pitfalls. *Neuroimage*. 2013;81:335-346.
26. Basser PJ, Pajevic S, Pierpaoli C, Duda J, Aldroubi A. In vivo fiber Tractography using DT-MRI data. *Magn Reson Med*. 2000;44:625-632.
27. Leemans A, Jeurissen B, Sijbers J, Jones D. ExploreDTI: a graphical toolbox for processing, analyzing, and visualizing diffusion MR data. *Magn Reson Med*. 2009;17(2):3537.
28. Ai T, Yu K, Gao L, et al. Diffusion tensor imaging in evaluation of thigh muscles in patients with polymyositis and dermatomyositis. *Br J Radiol*. 2014;87:20140261.
29. Li GD, Liang YY, Xu P, Ling J, Chen YM. Diffusion-tensor imaging of thigh muscles in Duchenne muscular dystrophy: correlation of apparent diffusion coefficient and fractional anisotropy values with fatty infiltration. *Am J Roentgenol*. 2016;206(4):867-870.
30. Ponrartana S, Ramos-Platt L, Wren TAL, et al. Effectiveness of diffusion tensor imaging in assessing disease severity in Duchenne muscular dystrophy: preliminary study. *Pediatr Radiol*. 2015;45(4):582-589.
31. Figueroa-Bonaparte S, Llauger J, Segovia S, et al. Quantitative muscle MRI to follow up late onset Pompe patients: a prospective study. *Sci Rep*. 2018;8(1):1-11.
32. Van Der Ploeg AT, Clemens PR, Corzo D, et al. A randomized study of alglucosidase alfa in late-onset Pompe's disease. *N Engl J Med*. 2010;362(15):1396-1406.
33. Van Zijl PCM, Jones CK, Ren J, Malloy CR, Sherry AD. MRI detection of glycogen in vivo by using chemical exchange saturation transfer imaging (glycoCEST). *Proc Natl Acad Sci U S A*. 2007;104(11):4359-4364.

SUPPORTING INFORMATION

Additional supporting information may be found online in the Supporting Information section at the end of this article.

How to cite this article: Rehmann R, Froeling M, Rohm M, et al. Diffusion tensor imaging reveals changes in non-fat infiltrated muscles in late onset Pompe disease. *Muscle & Nerve*. 2020;62:541–549. https://doi.org/10.1002/mus.27021